

# A CFD Study of the Fluid Flow through Air Distribution Hoses in a Greenhouse

Sigurd Sannan<sup>a,\*</sup>, Ionuț Ovidiu Jerca<sup>b</sup>, Liliana Aurelia Bădulescu<sup>b</sup>

<sup>a</sup> SINTEF Energy Reserach, P.O. Box 4761 Torgarden, NO-7465 Trondheim, Norway

<sup>b</sup> University of Agronomic Sciences and Veterinary Medicine of Bucharest, 59 Mărăști Boulevard, District 1, Bucharest, 011464, Romania  
[sigurd.sannan@sintef.no](mailto:sigurd.sannan@sintef.no)

The indoor climate of a greenhouse provides the plants with favorable growing conditions that can result in faster growth and higher yields. Important parameters to control in a greenhouse are the temperature, the humidity, and the level of CO<sub>2</sub> concentrations. In southern Europe, both heating and cooling are required to control the greenhouse temperatures throughout the year. In this study, Computational Fluid Dynamics (CFD) simulations is employed to study the fluid flow through air distribution hoses (ADHs) in a research greenhouse in Bucharest, Romania. The ADHs are part of a novel, energy-efficient concept at the greenhouse, comprised of an integrated heat pump system, air handling units (AHUs), a dry cooler, and borehole thermal energy storage. The heat pump system provides both heating and cooling, while the greenhouse humidity is controlled by the AHUs. CO<sub>2</sub>-enrichment to the greenhouse is provided from installed CO<sub>2</sub> tanks. The CO<sub>2</sub>-enriched air is circulated from the AHUs to the ADHs, which have a series of perforated holes along their lengths. In these preliminary simulations, different configurations of the perforated holes are simulated to optimize the mixing of the climate-controlled air with the greenhouse air. Both the diameters of the holes and the opening of the ADH outlet are varied to study the mass flow rates out of the holes. The CFD simulations provide suitable design criteria for the installation of ADHs in a greenhouse environment and for optimizing the efficiency of ADHs.

## 1. Introduction

Agricultural production is a major contributor to global anthropogenic greenhouse gas (GHG) emissions. Thus, the Food and Agriculture Organization of the United Nations estimates that agriculture and related land use emissions account for about 17% of the total global GHG emissions (FAO, 2021). This has a significant impact on global warming and climate change.

Meanwhile, agriculture is vulnerable to climate change and is in turn adversely affected by its consequences. Increased temperatures, changes in precipitation patterns and more frequent occurrences of extreme weather events, such as droughts or floods, are already negatively impacting crop production and pose a threat to global food security. In some regions, sea-level rise and increased salinity also lead to reduced crop yields.

On this background, the pressure on agricultural food systems is expected to increase in the coming years. This is intensified by the global population growth, which requires a substantial increase in food production by 2050 (Dijk, 2021). Sustainable food and nutrition security is therefore a major global issue which must be addressed through comprehensive measures taking the entire food system into account (FAO, 2018). Among several necessary steps, this includes efforts to reduce GHG emissions from agriculture, improved systems for water management, better soil conservation practices, use of advanced technologies for efficient monitoring and operation, and better solutions for reducing food waste.

Greenhouses are structures for growing fruit and vegetables that can help addressing the need for food production in the world (Kanwar, 2013). They can help reducing GHG emissions from agriculture by reducing the use of fertilizers, pesticides and water, and by enabling the cultivation of crops in a more controlled environment (Rabbi, 2019). Greenhouses also enable extended growing seasons and protect the crops from extreme weather conditions and pests, thereby increasing the yields (Ghoulem, 2019). In addition, due to that

greenhouses require less space than outdoor farming and can be located close to urban areas and local markets, greenhouse farming can help to reduce carbon footprints by minimizing the need for transportation. To provide the desired indoor climate for the plants in a greenhouse, however, greenhouses consume large amounts of energy for heating, cooling, ventilation, and lighting. In some cases, the energy consumption of a greenhouse can account for up to 50% of the total greenhouse costs for production (Shen, 2018). For farmers, energy-efficient operation of the greenhouses is therefore crucial, both for reducing costs and increasing the productivity.

Optimal growing conditions for the greenhouse plants require precise control of the temperature, humidity and CO<sub>2</sub> concentrations in the greenhouse, in addition to a suitable lighting system. In northern European countries, large heating demands are often required for controlling the temperature (Paris, 2022), while in southern parts of Europe both heating and cooling are required to control greenhouse temperatures throughout the year (Baptista, 2012). Especially, with global warming and hot summers in recent years (Copernicus, 2022), the need for efficient greenhouse cooling and humidity control becomes more and more important in many countries (Soussi, 2022).

In this paper, a CFD study of the air flow through air distribution hoses (ADHs) in a glass greenhouse located in Bucharest, Romania is presented. The greenhouse is used for research and horticultural growth studies at the University of Agronomic Sciences and Veterinary Medicine of Bucharest (USAMV), and the main challenge of the greenhouse is to provide sufficient cooling during the hot summer months. With daytime ambient temperatures occasionally reaching 35-40 °C in July and August, measurements have shown that the indoor greenhouse temperature can rise to 60 °C or more in the summertime.

The ADHs are part of a novel energy-efficient concept being installed at the greenhouse, consisting of an integrated heat pump system, air handling units (AHUs), borehole thermal energy storage (BTES), and a dry cooler (Brækken, 2023). The installed heat pumps are dimensioned to provide sufficient heating and cooling to the greenhouse, while the humidity is controlled by the AHUs and an already installed fogging system. CO<sub>2</sub> enrichment to the greenhouse compartments will be provided from CO<sub>2</sub> tanks in the new system. The BTES will be used for storing excess heat during the summer in the ground for winter usage. The borehole park at the current stage of installation consists of 15 boreholes, each with a depth of 110 m. The novel concept represents a shift towards a renewable and more environment-friendly energy system, replacing a gas-fired boiler currently being used both for heating and generation of CO<sub>2</sub> for the greenhouse plants.

In the physical setup of the new system, CO<sub>2</sub>-enriched air is distributed from the AHUs to the ADHs which have a series of perforated holes along their lengths. By varying the diameters of the holes, the current study simulates the mass flow rates out of the holes. The study presents work in progress and is performed to aid in the design of the ADHs to optimize the air throw and mixing of the climate-controlled air with the existing greenhouse air along the lengths of the ADHs.

## 2. Method

The greenhouse in this study has a total surface area of 2,756 m<sup>2</sup> and is structured into 19 integrated greenhouse compartments, of which there are 8 compartments of 160 m<sup>2</sup>, 10 compartments of 64 m<sup>2</sup>, and a smaller research room of 32 m<sup>2</sup>. In addition, there is an office, a technical area, and sanitation facilities. The greenhouse is equipped with advanced and automated systems for controlling the indoor climate and optimizing the conditions for a variety of fruits, vegetables and flowers growing in the greenhouse.

In the novel energy concept, two AHUs are being installed in each of the larger 160 m<sup>2</sup> compartments, while one AHU will be installed in each of the smaller compartments. The AHUs control the humidity by condensing cooling coils, while a fogging system is utilized when the compartment humidities fall to unsatisfactory low levels for the plants. In the larger compartments, three ADHs are connected to each of the AHUs for a total of six ADHs in each of these compartments. In these compartments, the focus is on studies of tomato plants and their growth conditions. The ADHs are installed underneath the tomato-growing benches and stretch along the length of the compartments.

### 2.1 ANSYS Fluent

In the current work, CFD simulations of the fluid flow through one ADH placed in one of the larger 160 m<sup>2</sup> compartments have been performed using the ANSYS Fluent 2022 R1 flow solver. The simulations are based on the Reynolds Averaged Navier-Stokes (RANS) equations, and for simplicity the computational domain is restricted to half of the compartment with one installed ADH. The computational domain of the simulations is shown in Figure 1, and a hexahedral mesh has been employed for the domain with about  $2.1 \times 10^6$  grid cells.

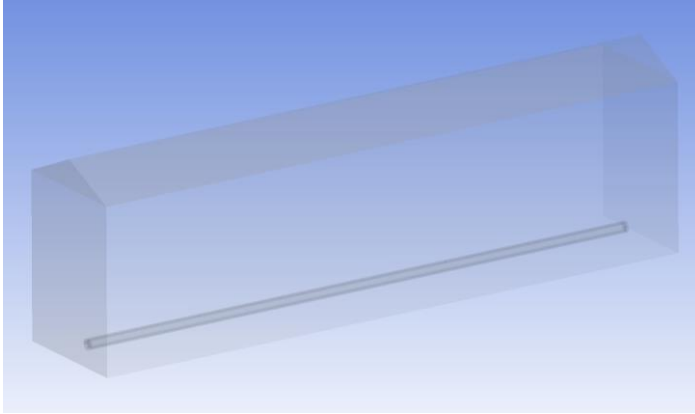


Figure 1: The computational domain with one air distribution hose.

Figure 2 shows the meshing of the ADH. The ADH has 26 pairs of perforated holes along the length of the hose, located at 10 a.m. and 2 p.m., respectively. For the simulations presented here, the diameters of the holes are varied in the range 20-30 mm to investigate the difference between holes of constant or varying diameter along the length of the air hoses. The distance between the pairs of the holes is 72 cm.

The length of the ADH is 18.7 m and the inner diameter is 28 cm. At the ADH inlet, the Fluent 3D Fan Zone model is employed, which simulates the effect of an axial fan. The fan inlet has a diameter of 24 cm, the fan hub radius is 4 cm, and the radius of the fan blade tips is 12 cm. The angular velocity of the fan is 20 rad/s, and the pressure jump across the 3D fan is 100 Pa. The settings of the fan zone give an air flow rate of about 900 m<sup>3</sup>/h, corresponding to one flow-through time for the air volume in the greenhouse compartment per hour. At the ADH outlet, a circular opening with variable opening size has been used. The opening is at the center of the outlet, and for the current simulations a diameter of 8 and 6 cm, respectively, has been applied for the opening.

The following specifications have been selected for the ANSYS Fluent simulation of the ADH configuration. The pressure-based Navier-Stokes solution algorithm is employed, together with the transient option, specifying that a time-dependent flow is being solved. The viscous model is specified by the realizable k- $\epsilon$  turbulence model, which predicts the spreading rate of jets more accurately than the standard k- $\epsilon$  model. For the pressure-velocity coupling, the SIMPLE scheme is used. For spatial discretization, the second order upwind scheme is selected for the momentum, continuity, and energy equation, where the latter is activated by choosing the ideal gas model for the air. For the equations of turbulent kinetic energy  $k$  and turbulent dissipation rate  $\epsilon$ , the first order upwind schemes are selected.



Figure 2: The meshed ADH shows the dense meshing around the perforated holes of the hose. The fan inlet at the end is shown in green.

### 3. Results and discussion

The results of the Fluent simulations of the fluid flow through the ADH are presented here. Figure 3a shows the velocity magnitude and Figure 3b shows the velocity vectors (right) of the air jets emanating from the perforated holes of the ADHs. The illustrations show that the velocities of the emerging jets tend to vary along the length of the air hoses, depending on the variation of the diameters of the holes along the hoses.

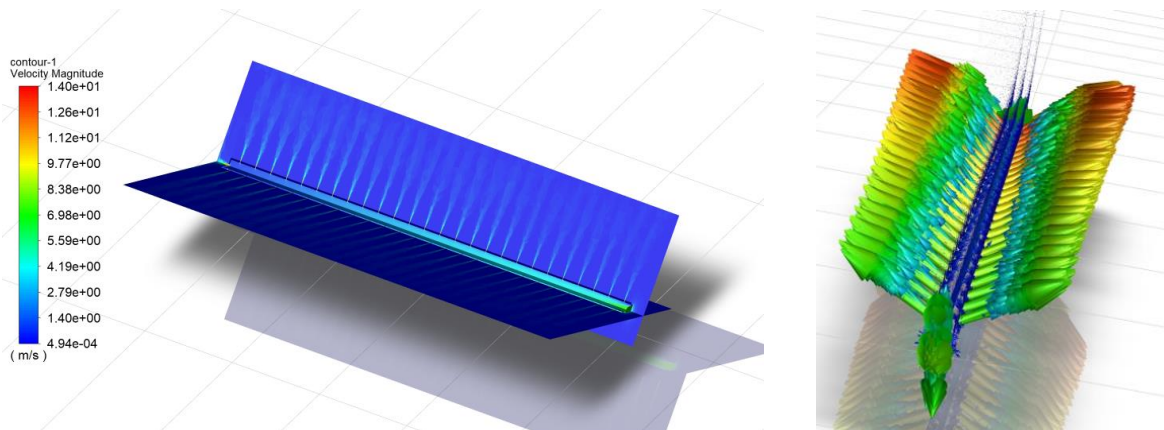


Figure 3: a) Contour plot of the velocity magnitude of the air jets emerging from the perforated holes of the ADH (left). b) The velocity vectors of the jets emanating from the holes (right).

Figure 4 shows the mass flow rates through the pairs of perforated holes of the ADH for various diameters of the holes and sizing of the ADH outlet. There are 26 pairs of holes along the ADH, and the figure shows the added mass flow rates of air jets through the pairs 1, 6, 11, 16, 21 and 26 of the ADH, as numbered from the ADH inlet to the outlet. For the two simulations indicated by "8 cm outlet – 1 inch holes" and "6 cm outlet – 1 inch holes", respectively, the diameters of the holes are kept constant at 1 inch (25.4 mm), while the diameter of the opening at the ADH outlet is varied between 8 and 6 cm. The corresponding graphs both show a drop in the mass flow rates from the first to the last pairs of holes along the ADH, calculated to be about 8.3% in both cases. As expected, the mass flow rates through the pairs of holes are correspondingly higher for the smaller sizing of opening (6 cm) compared to the larger sizing of the opening (8 cm). However, due to the relatively high number of hole pairs (26), the average mass flow rate through each of the hole pairs is only 2.1% higher for the 6 cm opening compared to the 8 cm opening.

In the second series of simulations shown in Figure 4, the diameters of the pairs of holes are increased stepwise from 20 to 30 mm, while the sizing of the ADH is varied between 8 and 6 cm. The corresponding legends "8 cm outlet – 20, 25, 30 mm holes" and "6 cm outlet – 20, 25, 30 mm holes" indicate that the diameters of the first 9 pairs of holes are kept constant at 20 mm, the diameters of the next 9 pairs are kept constant at 25 mm, while the diameters of the last 8 pairs are kept constant at 30 mm. In this case, the simulations show a large increase in the mass flow rates as the diameters of the holes increase along the ADHs. For the 8 cm opening at the outlet, the results show a 79.5% increase in the mass flow rate from the first to the last pair of holes along the ADH, and a corresponding 71.9% increase for the 6 cm sizing of the outlet opening. In this series of simulations, the average mass flow rate through the pair of holes is 4.9% higher for the 6 cm sizing of the outlet opening compared to the 8 cm opening. As in the first series of simulations, it is noted here that the mass flow rate drops along the ADH for pairs of equal diameters, i.e., the mass flow rates drop from the first pair to the pair 6, from the pair 11 to the pair 16, and from the pair 21 to the last pair 26.

Figure 5 shows the mass flow rates through the pairs of perforated holes of the ADH for various diameters of the holes and a constant sizing of 6 cm for the opening of the ADH outlet. The plots for the constant 1-inch holes and the 20, 25, and 30 mm holes are the same as shown in Figure 4, while the additional plot in the figure shows the result of a stepwise increase from 24 to 26 mm for the diameters of the hole pairs. For this simulation, the diameters of the first 9 pairs of holes are kept constant at 24 mm, the diameters of the next 9 pairs are kept constant at 25 mm, while the diameters of the last 8 pairs are kept constant at 26 mm. Since the variation from 20 to 30 mm diameters of the holes resulted in a large increase in the mass flow rates out of the holes along the ADH, the final simulation was performed to investigate a more balanced increase of the hole diameters. The simulation shows that the mass flow rates out of the perforated holes stay relatively constant along the ADH, with a 2.0% increase in the flow rates from the first pair of holes to the 26<sup>th</sup> pair of holes at the other end.

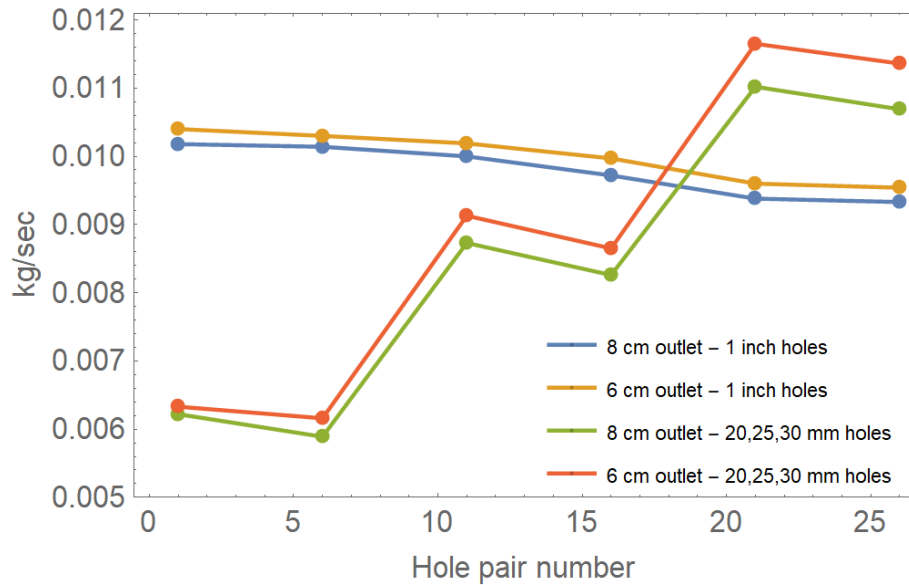


Figure 4: Mass flow rates through the pairs of perforated holes of the ADH for various diameters of the holes and sizing of the ADH outlet.

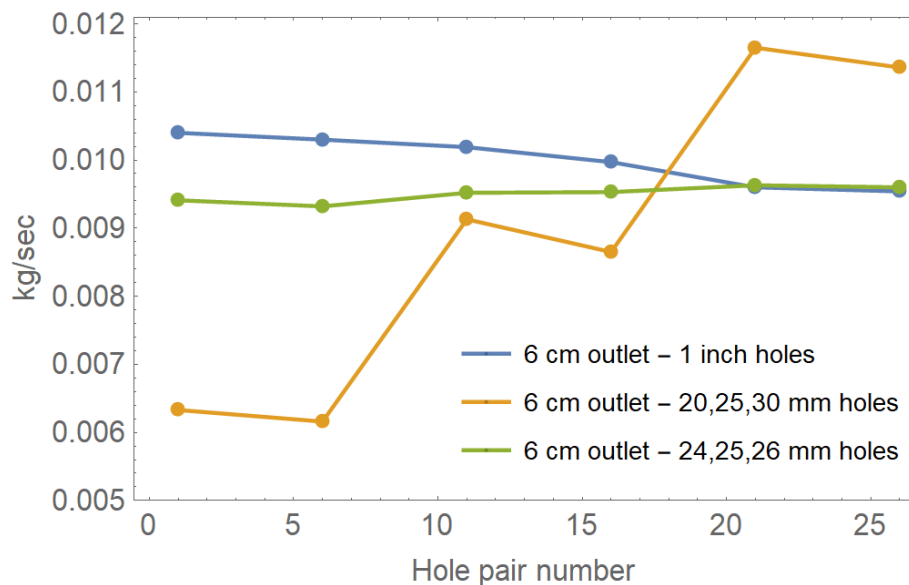


Figure 5: Mass flow rates through the pairs of perforated holes of the ADH for various diameters of the holes.

#### 4. Conclusions

In this work, a CFD study of the fluid flow through an air distribution hose installed in a glass greenhouse located in Bucharest, Romania has been performed. The simulated geometry corresponds to half of one of the 160 m<sup>2</sup> compartments of the greenhouse and is meshed with  $2.1 \times 10^6$  hexahedral grid cells. The simulations are based on the transient RANS equations, implying that a time-dependent flow was solved.

The installed AD is 18.7 m long, has an inner diameter of 28 cm, and is perforated with 26 pairs of holes along the length of its length. The pair of holes are located at 10 a.m. and 2 p.m., respectively. The ADH has an emulated fan zone at the inlet, with an air flow rate corresponding to one flow-through time for the air volume in the greenhouse compartment per hour.

The purpose of the study has been to investigate the impact of varying the diameters of the perforated holes along the length of the ADH. The initial simulations showed that a constant diameter of 1 inch (25.4 mm) resulted in a drop of 8.3% of the mass flow rate from the first to the last pair of holes along the ADH. To study the effect

of varying hole diameters, the diameters of the holes were increased stepwise from 20 to 30 mm along the ADH. The results of these simulations, both for an 8 and 6 cm opening at the outlet, showed a substantial increase of the mass flow rates out of the holes as their diameters increased along the ADH. In the final simulation, a stepwise increase from 24 to 26 mm for the diameters of the hole pairs. In this case, the simulation showed a relatively constant mass flow rate out of the perforated holes along the ADH.

To provide equal climatic conditions for the plants in a greenhouse, it is important that the mixing of climate-controlled air with the already existing greenhouse air is optimized everywhere in the greenhouse. The use of ADHs have proven to be a practical such system, for example in a tomato-growing greenhouse. The current study has shown that a slight increase of the diameters of the perforated holes along the ADHs will be necessary to optimize the air throw and mixing of the emanating air jets with the greenhouse air.

The present study is work in progress and further studies will be performed to optimize the distribution of climate-controlled air in a greenhouse. One option that will be pursued is to investigate the performance of double-layered air distribution hoses. With two hoses of different diameters, where the smaller hose is resting or hanging inside the larger hose, a pressure chamber between the two is created which may avoid the pressure loss seen in a single layer ADH. The distribution and sizes of the perforated holes in such a set-up will be the subject of future work to optimize the efficiency of such ADHs.

### Nomenclature

ADH – Air distribution hose

AHU – Air handling unit

BTES – Borehole thermal energy storage

CFD – Computational fluid dynamics

GHG – Greenhouse gas

Pa – Pascal

RANS – Reynolds Averaged Navier-Stokes

SIMPLE – Semi-Implicit Method for Pressure  
Linked Equations

USAMV – University of Agronomic Sciences and  
Veterinary Medicine of Bucharest

### Acknowledgments

The research leading to these results has received funding from the NO Grants 2014-2021, under Project contract no. 40/2021.

### References

- Baptista, F., Silva, A., Gracia, L.M., Correa-Guimaraes, A., Meneses, J., Greenhouse energy consumption for tomato production in the Iberian peninsula countries, 2012, *Acta Horticulturae*, 952, 409-416.
- Brækken, A., Sannan, S., Jerca, I.O., Bădulescu, L.A., 2023, Assessment of heating and cooling demands of a glass greenhouse in Bucharest, Romania, *Thermal Science and Engineering Progress*, 41, 101830.
- Copernicus, 2022, Globally, the seven hottest years on record were the last seven: carbon dioxide and methane concentrations continue to rise, <<https://climate.copernicus.eu/copernicus-globally-seven-hottest-years-record-were-last-seven>> accessed 15.05.2023
- Dijk, M. van, Morley, T., Rau, M.L., Saghai, Y., 2021, A meta-analysis of projected global food demand and population at risk of hunger for the period 2010-2050, *Nature Food*, 2, 494-501.
- FAO, 2021, Emissions due to agriculture. Global, regional and country trends, 1990-2018, FAOSTAT Analytical Brief Series No. 18. Rome.
- FAO, 2018, The future of food and agriculture – alternative pathways to 2050, Licence CC BY-NC-SA 3.0 IGO.
- Ghoulam, M., El Moueddeb, K., Nehdi, E., Boukhanouf, R., Calautit, J.K., 2019, Greenhouse design and cooling technologies for sustainable food cultivation in hot climates: Review of current practice and future status, *Biosystems Engineering*, 183, 121-150.
- Kanwar, M., 2013, Performance of tomato under greenhouse and open field conditions in the trans-Himalayan region of India, *Advances in Horticultural Science*, 25, 65-68.
- Paris, B., Vandorou, F., Balafoutis, A.T., Vaiopoulos, K. Kyriakarakos, G., Manolakos, D., Papadakis, G., 2022, Energy use in greenhouses in the EU: A review recommending energy efficiency measures and renewable energy sources adoption, *Applied Sciences*, 12, 5150.
- Rabbi, B., Chen, Z.-H., Sethuvenkatraman, S., 2019, Protected cropping in warm climates: A review of humidity control and cooling methods, *Energies*, 12, 2737.
- Shen, Y., Wei, R., Xu, L., 2018, Energy consumption prediction of a greenhouse and optimization of daily average temperature, *Energies*, 11, 65.
- Soussi, M., Chaibi, M.T., Buchholz, M., Saghrouni, Z., 2022, Comprehensive review on climate control and cooling systems in greenhouses under hot and arid conditions, *Agronomy*, 12, 626.